

Effectively Investigating Dark Matter Microphysics With Strong Gravitational Lensing Anisotropies

Birendra Dhanasingham 

Department of Physics and Astronomy, University of New Mexico, 210 Yale Blvd NE,
Albuquerque, NM 87106, USA. email: birendradh@unm.edu

Abstract. Over the last two decades, strong gravitational lensing has emerged as a potential method for studying the nature and distribution of dark matter on sub-galactic scales. In addition to the main lens substructure, line-of-sight dark matter haloes contribute greatly to the subtle perturbations of lensed images. Line-of-sight haloes, unlike dark matter subhaloes, imprint distinct anisotropic and quadrupole signatures in the maps that depict the divergence and curl of the effective deflection field, respectively, giving rise to quadrupole moments of the image-plane averaged two-point correlation function of these maps. In terms of central density evolution and dark matter halo distribution, the shapes and amplitudes of the two-point function multipoles alter dramatically in the presence of warm dark matter and self-interacting dark matter. This method, in conjunction with upcoming large-scale surveys, provides the prospect of improving the constraints on dark matter at a critical time in strong gravitational lensing research.

Keywords. gravitational lensing; strong – galaxies: haloes – methods: numerical – dark matter

1. Introduction

Dark matter plays a critical role in the hierarchical structure formation in the classic cold dark matter (CDM) model, where dark matter is spread into haloes with a wide range of masses. While the largest haloes are known to contain clusters and galaxies and hence are luminous, the smallest haloes have a relatively Weak gravitational potential to hold gases and thus are dark. The investigation of such dark haloes, particularly on small distance scales, might give answers to the inadequacy of the Lambda-CDM model's success deep in the non-linear regime.

Strong gravitational lensing is a unique method for studying dark matter haloes at sub-galactic distance scales. [Dhanasingham *et al.* \(2023a\)](#) pointed out that line-of-sight dark matter haloes located between the lensed source and the observer produce a distinct anisotropic signature in the two-point correlation function of the lensing deflection field when considering the collective effect of multiplane gravitational lens planes. I summarize here this anisotropic correlation function approach presented by [Dhanasingham *et al.* \(2023a\)](#) as a potential probe of dark matter, as well as how this function behaves in the presence of different dark matter physics, as discussed in [Dhanasingham *et al.* \(2023b\)](#).

2. Effective Multiplane Lensing

Photons are deflected repeatedly by dark matter haloes as they travel across the Universe from a background source to an observer. This multiplane lensing is often handled using a recursive technique that involves solving a lens equation for each lens plane

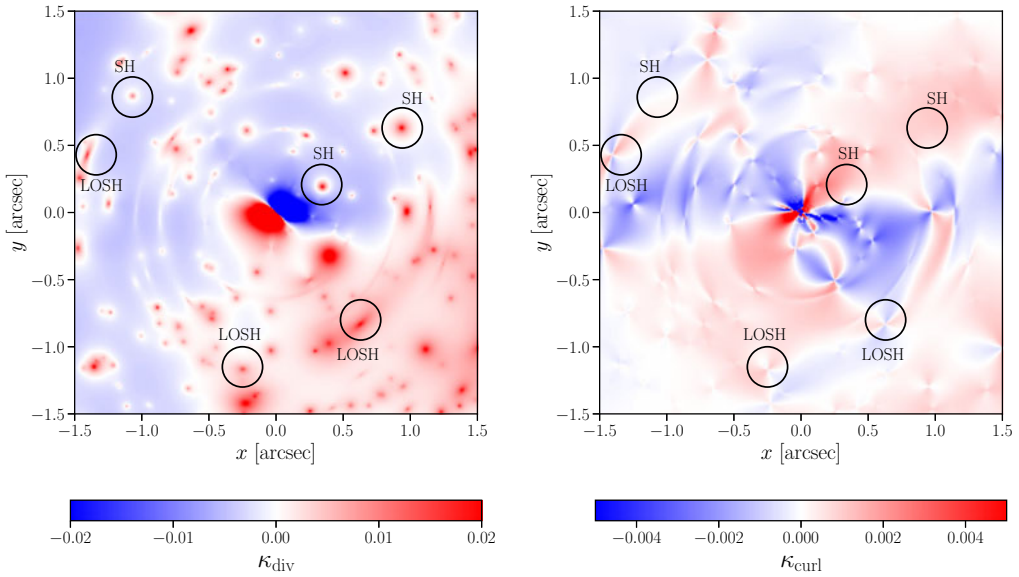


Figure 1. Divergence (left) and curl (right) of the effective deflection field for a CDM model, incorporating contributions from subhaloes (SH) and line-of-sight haloes (LOSH). On the left, line-of-sight haloes seem deformed in the angular direction, although subhaloes are mainly circular, and on the right, these line-of-sight haloes are accompanied by quadrupolar structures, whereas subhaloes contribute nothing to this map. Figure from [Dhanasingham *et al.* \(2023b\)](#).

([Blandford & Narayan 1986](#); [McCully *et al.* 2014](#)). Lensing, on the other hand, is intrinsically a two-dimensional map from the source plane to the image plane. This map may be written as a pure gradient of some scalar lensing potential in the single-plane case. Because of the nonlinear coupling between the multiple lens planes, this map is no longer a pure gradient for multiplane lensing. [Dhanasingham *et al.* \(2023a\)](#) thus proposed a novel approach named “effective multiplane lensing” that took into account the collective influence of all the lens planes in the strong lens system, where one scalar (ϕ_{eff}) and one vector (\mathbf{A}_{eff}) effective potential were included to write down the effective deflection field

$$\boldsymbol{\alpha}_{\text{eff}}(\mathbf{x}) = \nabla\phi_{\text{eff}}(\mathbf{x}) + \nabla \times \mathbf{A}_{\text{eff}}(\mathbf{x}), \quad (1)$$

and thus the lens equation

$$\mathbf{u}(\mathbf{x}) = \mathbf{x} - \boldsymbol{\alpha}_{\text{eff}}(\mathbf{x}), \quad (2)$$

where \mathbf{u} and \mathbf{x} are the source plane and image plane coordinate systems, respectively. This decomposition of the effective deflection field is based on Helmholtz’s theorem. Without any approximation, the two effective scalar and vector potentials encode the full nonlinear multiplane lensing map from the source plane to the image plane. In this terminology, the two forms of two-dimensional projected mass densities are defined as $\kappa_{\text{div}} \equiv \frac{1}{2}\nabla \cdot \boldsymbol{\alpha}_{\text{eff}} - \kappa_0$ and $\kappa_{\text{curl}} \equiv \frac{1}{2}\nabla \times \boldsymbol{\alpha}_{\text{eff}} \cdot \hat{\mathbf{z}}$, taking into account the divergence and curl of the effective deflection field ([Gilman *et al.* 2019](#); [Çağan Şengül *et al.* 2020](#); [Dhanasingham *et al.* 2023a](#)). To distinguish the collective effect from dark matter haloes, the main lens convergence κ_0 is deducted from the κ_{div} equation. Figure 1 depicts the κ_{div} and κ_{curl} for a CDM model.

As seen in the left panel of Figure 1, Line-of-sight haloes appear stretched in the tangential direction and generate arc-like patterns due to the distortion on their deflection field caused by the main lens due to the non-linear nature of multiplane gravitational

lensing. While these distortions contribute anisotropic signals to the κ_{div} map, subhaloes still seem circular and hence stay isotropic in the κ_{div} map. When comparing the κ_{div} and κ_{curl} maps, one can see quadrupolar patterns in the right panel at the sites of line-of-sight haloes. These anisotropic and quadrupolar fingerprints, as proposed by [Dhanasingham et al. \(2023a\)](#), can be utilized to identify line-of-sight dark matter haloes from the main lens substructure and study dark matter microphysics of these haloes. [Dhanasingham et al. \(2023a,b\)](#) proposed a method for capturing the useful information encoded in these signatures based on the two-point correlation function and its breakdown into multipoles, as described in the next section.

2.1. Two-point Correlation Functions and Multipoles

As previously noted, the existence of line-of-sight haloes causes a noticeable anisotropy between the tangential and radial directions in the divergence of the effective deflection field and the quadrupolar patterns in the curl of the deflection field. Because of these anisotropies and quadrupoles, the image-plane averaged two-point functions of the κ_{div} and κ_{curl} fields have non-vanishing quadrupole moments ([Dhanasingham et al. 2023a,b](#)). The two-point function for a given κ (represents either κ_{div} or κ_{curl}) is denoted as:

$$\xi(\mathbf{r}) = \frac{1}{A} \int_A d^2\mathbf{r}_1 [\kappa(\mathbf{r}_1) - \langle \kappa(\mathbf{r}_1) \rangle] [\kappa(\mathbf{r}_2) - \langle \kappa(\mathbf{r}_2) \rangle], \tag{3}$$

where \mathbf{r}_1 and $\mathbf{r}_2 = \mathbf{r}_1 + \mathbf{r}$ are the position vectors of two points on the map connected by vector \mathbf{r} , and the A is the area of the image where the correlation is computed. The multipole decompositions for the two-point functions of the κ_{div} and κ_{curl} maps are given by

$$\xi_{\text{div},\ell}(r) = \frac{2 - \delta_{\ell 0}}{\pi} \int_0^\pi d\theta \xi_{\text{div}}(r, \theta) \cos(\ell\theta) \tag{4}$$

and

$$\xi_{\text{curl},\ell}(r) = \frac{2}{\pi} \int_0^\pi d\theta \xi_{\text{curl}}(r, \theta) A_\theta \sin(\ell\theta), \tag{5}$$

respectively. Here θ is the angle between \mathbf{r} and radial direction and δ_{ij} is the Kronecker delta. The parameter $A_\theta = \begin{cases} +1 & 0 \leq \theta < \frac{\pi}{2}, \\ -1 & \frac{\pi}{2} \leq \theta < \pi \end{cases}$ in equation (5) captures the useful information hidden in the odd-parity structure in the κ_{curl} map, as detailed in [Dhanasingham et al. \(2023b\)](#).

Figure 2 depicts the multipole decompositions of the two-point correlation function of the projected mass densities κ_{div} and κ_{curl} for a population of CDM subhaloes and line-of-sight haloes following this approach. The statistical features of the main-lens subhaloes are completely represented by a monopole ($\ell = 0$) term (showing no anisotropy), but the line-of-sight haloes contribute to both the monopole and the quadrupole ($\ell = 2$) moments as shown in the left panel. This quadrupole moment represents the anisotropies in the deflection field perturbation induced by line-of-sight haloes between the tangential and radial directions. Using Fisher forecasting, [Dhanasingham et al. \(2023a\)](#) pointed out that present space-based telescopes and future extremely large telescopes may identify the quadrupole signal. Because the main lens substructure makes no contribution to the κ_{curl} map, the non-zero quadrupole moment presented in the right panel solely reflects the statistical features of the line-of-sight haloes ([Dhanasingham et al. 2023b](#)).

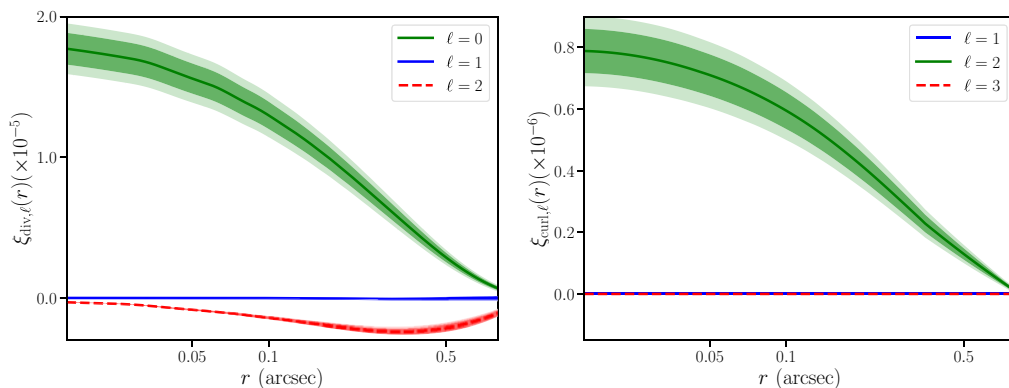


Figure 2. Multipole moments of the two-point correlation function of a CDM model's κ_{div} (left) and κ_{curl} (right) fields. On the left panel, the monopole is formed by both the line-of-sight haloes and the primary lens substructure, but the non-zero quadrupole is formed only by the line-of-sight haloes. The non-zero quadrupole moment in the right panel is entirely due to the line-of-sight haloes.

3. Multipoles and Dark Matter Microphysics

Dhanasingham *et al.* (2023b) investigated the use of two-point function multipoles as a probe of dark matter from two perspectives: first, they investigated how the shapes and amplitudes of multipoles change with the evolution of the central density in self-interacting dark matter (SIDM) haloes, and second, they investigated how the abundance of dark matter haloes affects the multipoles in warm dark matter models. I describe their findings in this section.

3.1. Self-interacting Dark Matter (SIDM)

By enabling dark matter particles to interchange energy and momentum, self-interactions can radically modify the internal dynamics of haloes. Initially, a Navarro-Frenk-White (NFW) (Navarro *et al.* 1996) halo has a high temperature close to the outer skirts, so heat flows inward and particles flow outward due to dark matter particle self-interaction until a low-density isothermal core forms, and this core, with its high temperature relative to the outer skirts, now favors an outward heat flow. The isothermal core eventually begins to shrink, resulting in a sharp density cusp. When compared to cored haloes, these core-collapsed haloes serve as excellent lenses. The number of core-collapsed haloes grows as the self-interaction cross-section increases, but the central densities of cored haloes drop due to the high rate of outward mass flow.

The correlation function multipoles of the κ_{div} and κ_{curl} maps for SIDM models are shown in the left panel of Figure 3 as a function of the self-interaction cross-section, σ ($\propto \sigma_0$). When σ is small, cored haloes dominate the amplitudes of the multipoles of the two-point functions, resulting in a lower relative amplitude than the CDM model. As σ increases, subhaloes can begin to core-collapse, resulting in a steeper and stronger monopole ($\xi_{\text{div},0}$) for lower r values, but line-of-sight haloes are still cored, resulting in comparatively suppressed quadrupole ($\xi_{\text{div},2}$) compared to the CDM model. Subhaloes and line-of-sight haloes both experience core-collapse as σ further increases, causing $\xi_{\text{div},0}$ and $\xi_{\text{div},2}$ to grow large and steep at small r values. In addition, due to the core-collapsed line-of-sight haloes, quadrupole, $\xi_{\text{curl},2}$, exhibits a slight amplitude increase at small r . As a result, it is obvious that the monopole and quadrupole moments of the correlation function multipoles could be used to investigate dark matter self-interactions.

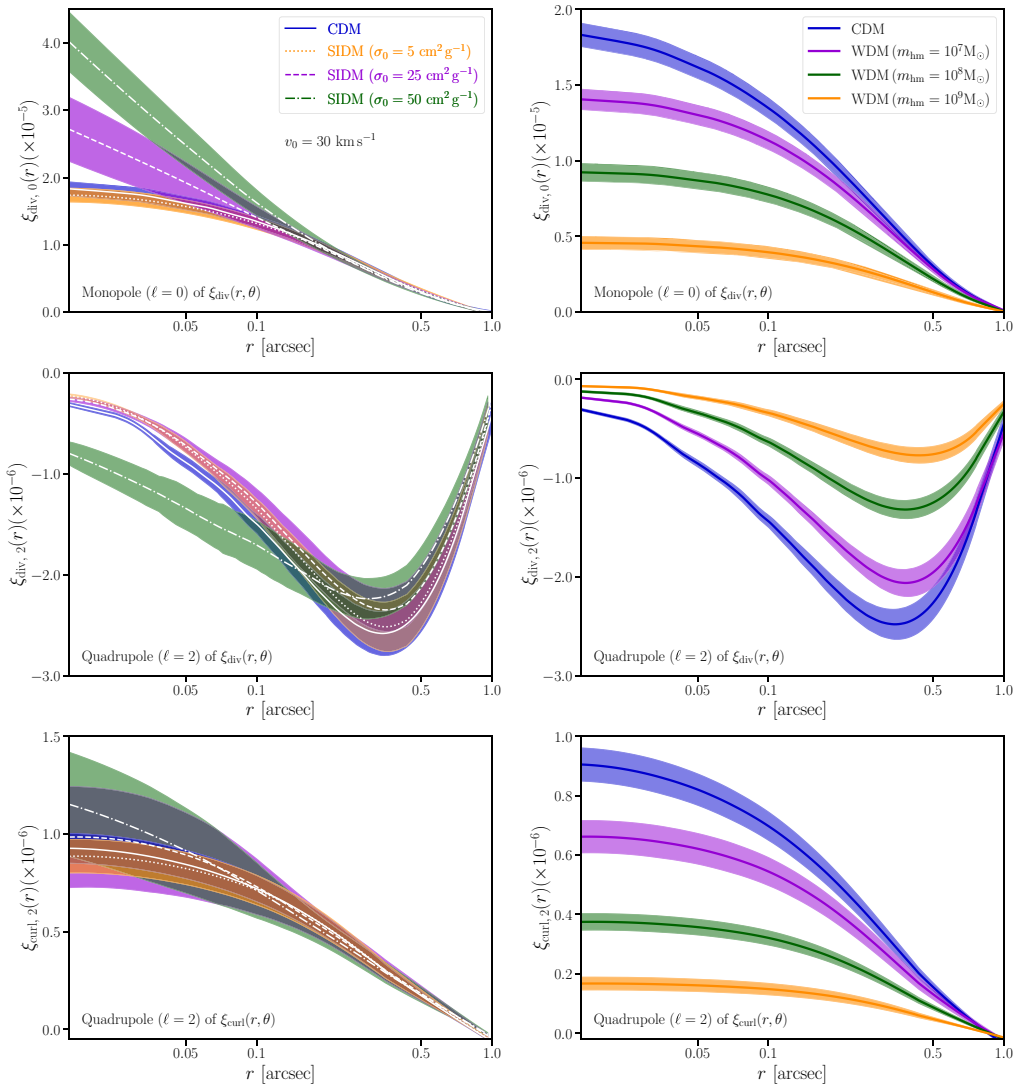


Figure 3. The monopole (top panel) and the quadrupole (middle panel) of the two-point correlation function ξ_{div} , and the quadrupole (bottom panel) of the ξ_{curl} function for SIDM (left panel) and WDM (right panel) models. The coloured regions represent the 68% credible intervals. The amplitude and shapes of the multipoles are principally determined by the evolution of the central density in SIDM models and the abundance in WDM models. Figure from [Dhanasingham et al. \(2023b\)](#).

3.2. Warm Dark Matter (WDM)

The right panel of Figure 3 depicts the correlation function multipoles of the κ_{div} and κ_{curl} maps for three WDM models. As the characteristic half-mode mass (m_{hm}) grows in WDM models, the abundance of dark matter haloes diminishes because free-streaming effects erase the structure below m_{hm} . The relative amplitudes of the multipoles fall as m_{hm} increases at small radial distances, reflecting the suppressed abundance of small haloes. The difference in amplitudes is small over large radial distances because the massive haloes that dominate these scales are less impacted by free-streaming effects.

As a result, the combination of quadrupole and monopole moments includes crucial information on the physics beneath the minuscule dark matter haloes. Observing it might put our traditional theory of structure formation to the test.

References

- Blandford, R. & Narayan, R. 1986, *ApJ*, 310, 568
- Çağan Şengül, A., Tsang, A., Diaz Rivero, A., Dvorkin, C., Zhu, H. & Seljak, U. 2020, *Phys. Rev. D*, 102, e063502
- Dhanasingham, B., Cyr-Racine, F., Peter, A., Benson, A. & Gilman, D. 2023, *MNRAS*, 518, 5843
- Dhanasingham, B., Cyr-Racine, F., Mace, C., Peter, A. & Benson, A. 2023, *MNRAS*, 526, 5455
- Gilman, D., Birrer, S., Treu, T., Nierenberg, A. & Benson, A. 2019, *MNRAS*, 487, 5721
- McCully, C., Keeton, C., Wong, K. & Zabludoff, A. 2014, *MNRAS*, 443, 3631
- Navarro, J., Frenk, C. & White, S. 1996, *ApJ*, 462, 563